IEICE Electronics Express, Vol.16, No.7, 1–4

LETTER

A filter design method based on higher-order modes of fan-shaped half-mode substrate integrated waveguide resonator

Sheng Zhang[1], **Jun-Jie Cheng**[1], **Ya Guo**[1], **Hai Liu**[1], **and Shou-Feng Tang**[1a)]

Abstract In this paper, a novel 22.5° fan-shaped half-mode substrate integrated waveguide resonator (FSHMSIWR) is presented firstly. Based on it, a filter design method by suppression or utilization of higher-order modes is proposed. When feeding on magnetic wall, the fundamental mode (TM_{101}) is excited to generate passband response, while the higher-order modes (TM_{201} and TM_{301}) can be suppressed. A pair of complementary split-ring resonators (CSRRs) are introduced to strengthen the out-band rejection. Then a single-band bandpass filter (BPF) with ultra-wide and deep stopband is realized. When feeding on electric wall, the higher-order modes can be well excited, which provides flexibility to realize multi-band BPFs only by changing the feeding position. As verification, a single-band BPF and a tri-band BPF with source-load coupling are designed and fabricated. The measured results show good agreement with the simulated ones.

Keywords: fan-shaped half-mode substrate integrated waveguide resonator (FSHMSIWR), single-band BPF, tri-band BPF, higher-order mode

Classification: Microwave and millimeter-wave devices, circuits, and modules

1. Introduction

Substrate integrated waveguide (SIW) technology has widely applied in bandpass filter (BPF) designs for its easy-integration, low-cost and high-quality factor [1, 2, 3, 4, 5, 6]. Especially SIW has been attractive to design multi-band BPFs [7, 8, 9, 10, 11]. In general, the design method is combining several single-band BPFs at different frequencies to form the multi-band response [12, 13, 14], or cascading bandstop structures to divide a wide passband into multiple passbands [15, 16]. However, the sizes are large and the design procedures are complex. For miniaturization, half-mode and one-third mode SIW resonators are proposed [17, 18], but few are used to develop multi-band BPF [19, 20, 21]. Recently, various SIW tri-mode resonators have been reported [22, 23, 24, 25], but it is hard to design tri-band BPF due to the difficulty in controlling the three modes [26]. In [27], a multilayer LTCC tri-band filter is designed, but the whole performance is poor and the fabrication is costly.

In this paper, a novel 22.5° fan-shaped half-mode substrate integrated waveguide resonator (FSHMSIWR) is firstly presented. According to its electric field distributions, a simple method for filter design is proposed. When feeding on magnetic wall, only TM_{101} mode is excited to generate passband response. The inductive window is properly adjusted to further suppress TM_{201} mode, which allows TM_{101} mode to be coupled together simultaneously. To better suppress TM_{301} mode, a pair of complementary split-ring resonators (CSRRs) are employed to produce one transmission zero (TZ) [28]. Hence, the higher-order modes are completely inhibited, which contributes to a single-band BPF with ultra-wide and deep upper stopband. When feeding on electric wall, TM_{101} and the higher-order modes are all excited well. Then, FSHMSIWR can act as multi-mode resonator to realize multi-band BPFs, which keeps the size compact rather than cascading additional resonators. To verify this, a tri-band BPF is designed. TM_{101}, TM_{201} and TM_{301} modes are utilized to generate three passbands, correspondingly. Source-load coupling is introduced to improve the out-band attenuation level [29]. As a result, the proposed method supplies a shortcut for designing single-band or tri-band filters only by changing the feeding position. Finally, the two BPFs are fabricated. The measured stopband of single-band BPF ranges from 5.37 GHz to 15.2 GHz with the attenuation better than 20-dB. The measured three passbands of tri-band BPF are located at 5.2, 7.44, 9.57 GHz, respectively. And total seven TZs are obtained and result in high selectivity out of band. The measured results agree well with the simulations.

2. FSHMSIWR

The electric field distribution for the TM_{101} mode of 22.5° FSHMSIWR is shown in Fig. 1, which is evolved from 45° fan-shaped SIW resonator (FSSIWR) by bisecting along the magnetic wall (O-O') of the cavity, and the arc side is electric wall (P-P'). According to [8] and the least square method, the resonant frequency of TM_{101} mode can be calculated as follows:

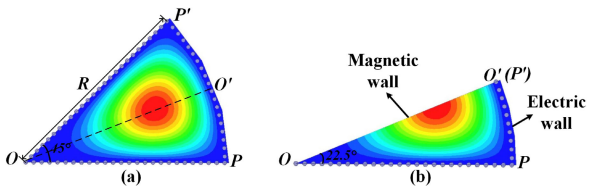

Fig. 1. (a) 45° FSSIWR (b) 22.5° FSHMSIWR.

[1]School of Information and Control Engineering, China University of Mining and Technology, Xuzhou, 221116, China

a) tsf0816@126.com

DOI: 10.1587/elex.16.20190039
Received January 22, 2019
Accepted February 19, 2019
Publicized March 11, 2019
Copyedited April 10, 2019

$$f_{TM_{101}} = \frac{1.25}{R}\frac{c}{\sqrt{\mu_r \varepsilon_r}}. \quad (1)$$

Where c is the speed of light in vacuum, μ_r and ε_r are relative permeability and relative permittivity. Fig. 2 shows the electric field distributions of TM_{101}, TM_{201} and TM_{301} modes, respectively. On the one hand, compared with TM_{101} mode, the electric field of TM_{201} and TM_{301} modes are relatively weak between adjacent half standing waves. If feeding on magnetic wall (O-O'), only TM_{101} mode is excited while the higher-order modes cannot be excited at the same time. On the other hand, the electric fields of three modes increase similarly along the arc side (P to P'). If feeding on electric wall (P-P'), TM_{101} and the higher-order modes can be excited well, simultaneously. According to that, FSHMSIWR is available to realize single-band or multi-band responses by changing the feeding position.

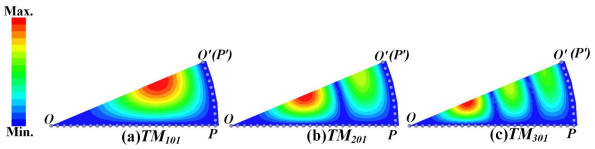

Fig. 2. Electric field distributions (a) TM_{101} (b) TM_{201} (c) TM_{301}.

3. Filters design

3.1 Single-band BPF

To verify the idea above, a single-band BPF is designed firstly as depicted in Fig. 3. Two FSHMSIWRs are cascaded through an inductive window. The 50 Ω microstrip lines are directly connected to magnetic walls as the input/output ports. The external quality factor (Q_e) can be calculated by [30]:

$$Q_e = \frac{2f_0}{\Delta f_{-3dB}}. \quad (2)$$

Where f_0 is the resonant frequency and Δf-3 dB is the 3-dB bandwidth. Fig. 4(a) shows the Q_e of TM_{101}, TM_{201} and TM_{301} modes (Q_e^1, Q_e^2 and Q_e^3) versus feeding position (S_0), Q_e^1, Q_e^2 and Q_e^3 change asynchronously as S_0 increases. It is indicated that when TM_{101} mode is excited with a suitable S_0 to generate the first passband, the two higher-order modes are not well excited and unavailable.

In Fig. 3(a), the location of inductive window 1 is adjusted to further suppress TM_{201} mode according to the electric field distribution of it. Meanwhile, TM_{101} mode can be coupled together by a suitable width of inductive window 1 (W_{12}). And slot coupling is used to enhance the coupling strength. The coupling coefficient (M_{12}) between two FSHMSIWRs can be calculated by [30]:

$$M_{12} = \frac{f_1^2 - f_2^2}{f_1^2 + f_2^2}. \quad (3)$$

Where f_1 and f_2 are the higher and lower resonant frequencies, respectively. Fig. 4(b) shows the M_{12} of TM_{101}, TM_{201} and TM_{301} modes (M_{12}^1, M_{12}^2 and M_{12}^3) versus W_{12}. It shows that a larger W_{12} could lead to the increases of M_{12}^1 and M_{12}^3, while M_{12}^2 keeps almost unchanged. Then, TM_{201} mode is completely suppressed by a proper inductive window. The simulated $|S_{21}|$ of the sing-band BPF are shown in Fig. 5. Nonetheless, the stopband performance degrades due to TM_{301} mode, which appears around 11 GHz. To further suppress it, a pair of rectangular CSRRs are etched on the ground to produce one TZ as shown in Fig. 3(b). Compared with the simulated $|S_{21}|$ without CSRRs, an ultra-wide and deep upper stopband can be achieved. The proposed single-band BPF is fabricated and shown in Fig. 6. The dielectric substrate is *RT/duroid* 6006 with $\varepsilon_r = 6.15$, and $tan\delta = 0.0019$, its thickness is $h = 0.635$ mm. The final optimized dimensions are as follows (all in mm): $R = 25$, $d = 0.5$, $p = 1$, $L_0 = 4$, $w_0 = 0.75$, $S_0 = 10.84$, $w_{12} = 3.4$, $L_{S1} = 3$, $L_{S2} = 0.8$, $L_C = 1.98$, $g = 0.2$, $a = b = c = 0.2$.

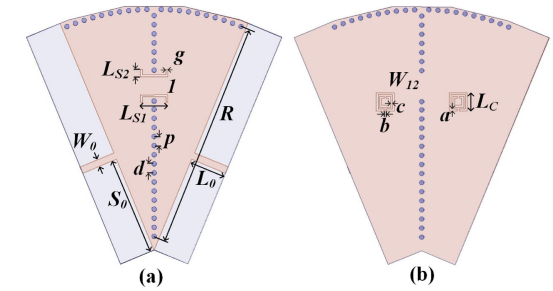

Fig. 3. Configuration of the single-band BPF (a) Top view (b) Bottom view.

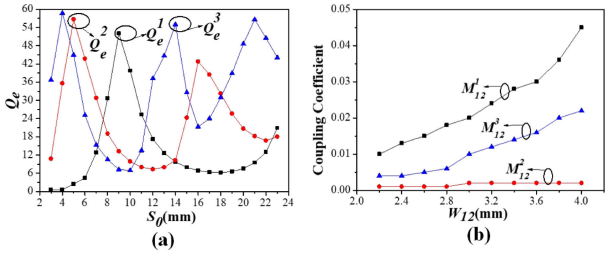

Fig. 4. (a) Q_e of the three modes (b) M_{12}^1, M_{12}^2 and M_{12}^3 versus W_{12}.

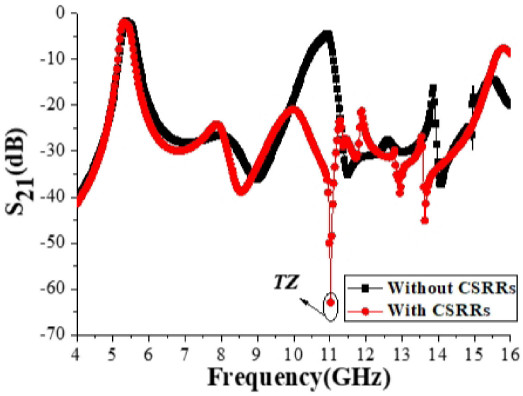

Fig. 5. Comparison of simulated $|S_{21}|$ with and without CSRRs.

The measured center frequency (f_0) is 5.37 GHz, and the 3-dB bandwidth is 210 MHz. The minimum $|S_{21}|$ is 1.91 dB. Since the higher-order modes have been inhibited,

the upper stopband is extended to $2.7f_0$ with the attenuation better than 20-dB. Some slight differences between the simulated and measured results may be caused by unavoidable tolerance in fabrication and measurement. Consequently, by feeding on magnetic wall, the sing-band BPF is easily designed and exhibits wide stopband and good rejection.

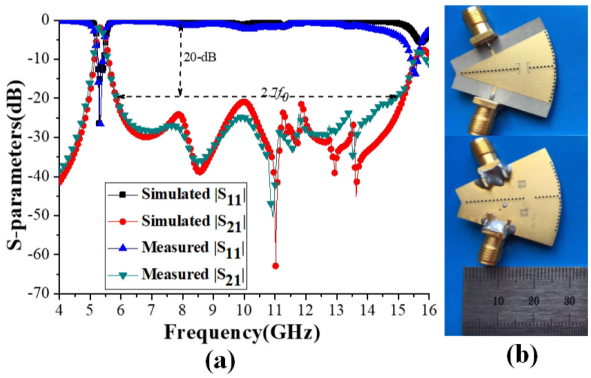

Fig. 6. (a) S-parameters (b) Photograph of the single-band BPF.

3.2 Tri-band BPF

When feeding on electric walls, FSHMSIWR is used as multi-mode resonator to realize multi-band responses. Typically, a tri-mode tri-band BPF is chosen to design as depicted in Fig. 7. Fig. 8(a) shows Q_e^1, Q_e^2 and Q_e^3 versus the coupling slot length (L_{S3}). Q_e^1, Q_e^2 and Q_e^3 decrease synchronously as L_{S3} increases, which indicate that TM_{101} and the higher-order modes all can be excited well with a suitable L_{S3} at the same time. Therefore, a tri-band response is feasible to realize by utilizing TM_{101}, TM_{201} and TM_{301} modes, correspondingly.

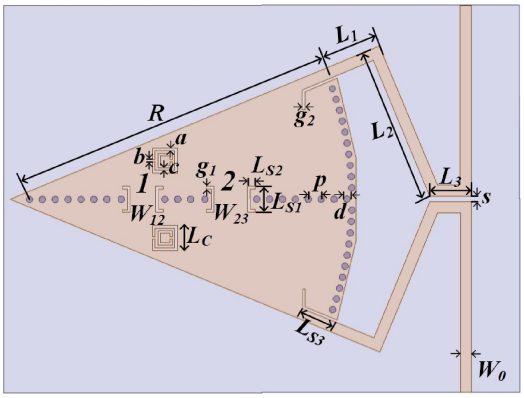

Fig. 7. Configuration of the tri-band BPF.

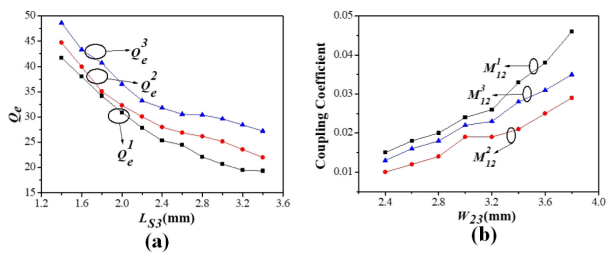

Fig. 8. (a) Q_e of the three modes (b) M_{12}^1, M_{12}^2 and M_{12}^3 versus W_{23} with fixed W_{12}.

Based on the electric field distributions, the inductive window 1 is rightly placed where all three modes can be coupled individually. In order to achieve the desired coupling strength, another inductive window 2 is introduced as shown in Fig. 7. Fig. 8(b) shows M_{12}^1, M_{12}^2 and M_{12}^3 versus the width of inductive window 2 (W_{23}) with fixed W_{12}. It is clear that M_{12}^1, M_{12}^2 and M_{12}^3 grow apparently with the increase of W_{23}.

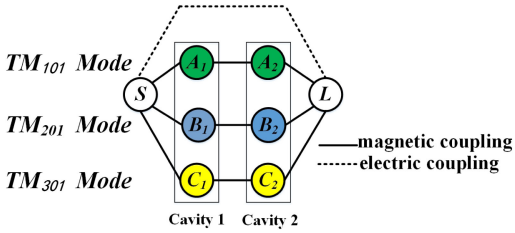

Fig. 9. Coupling scheme.

The coupling scheme of the tri-band BPF is shown in Fig. 9, $A_1(A_2)$, $B_1(B_2)$, $C_1(C_2)$ represent the TM_{101}, TM_{201} and TM_{301} modes in the first and second cavities, respectively. The three modes are magnetically coupled via three separate paths. Meanwhile, the source and load are electrically coupled directly. Then multiple TZs can be obtained to improve the out-band attenuation level. CSRRs are aimed to produce an extra TZ at the upper stopband. The final optimized dimensions are as follows (all in mm): $R = 25$, $d = 0.5$, $p = 1$, $w_0 = 0.85$, $w_{12} = 3.38$, $w_{23} = 4.02$, $L_1 = 4$, $L_2 = 13.2$, $L_3 = 3.2$, $L_{S1} = 2$, $L_{S2} = 0.6$, $L_{S3} = 2.82$, $L_C = 1.92$, $s = 0.45$, $g_1 = g_2 = 0.2$, $a = b = c = 0.2$.

As shown in Fig. 10, the measured three passbands are located at 5.2, 7.44, 9.57 GHz and the 3-dB bandwidths are 470, 790, 480 MHz, respectively. The measured minimum $|S_{21}|$ of the three passbands are 1.63, 1.95, 1.72 dB, respectively. The measured $|S_{11}|$ are all better than 15 dB. Total seven TZs are obtained, among which TZ7 is produced by CSRRs and the others (TZ1–TZ6) are attributed to the source-load coupling. It can be found that the tri-band BPF has the advantages of compact size and good return losses. Thus, FSHMSIWR is converted to tri-mode resonator only by changing the feeding position, which contributes to the miniaturization of tri-band BPF design.

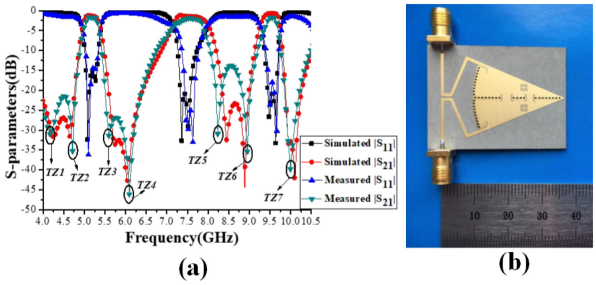

Fig. 10. (a) S-parameters (b) Photograph of the tri-band BPF.

4. Conclusion

In this paper, a simple method for filter design based on novel 22.5° FSHMSIWR is proposed and analyzed. When feeding on magnetic wall, a single-band BPF with ultra-wide and deep upper stopband is realized by suppression of higher-order modes. When feeding on electric wall, FSHMSIWR can act as multi-mode resonator. A tri-band BPF is realized by utilization of higher-order modes. CSRRs and source-load coupling are introduced to improve the out-band selectivity. Compact size and good filtering performance are achieved. The proposed method provides convenience and flexibility for filter design.

Acknowledgments

This work is supported by National Key R&D Program of China (2017YFF0205500).

References

[1] X. P. Chen, *et al.*: "Substrate integrated waveguide filter: Basic design rules and fundamental structure features," IEEE Microw. Mag. **15** (2014) 108 (DOI: 10.1109/MMM.2014.2321263).
[2] A. Sahu, *et al.*: "Recent advances in theory and applications of substrate integrated waveguides: A review," Int. J. RF Microw. Comput.-Aided Eng. **26** (2016) 129 (DOI: 10.1002/mmce.20946).
[3] A. Kumar, *et al.*: "A review on future planar transmission line," Cogent Eng. **3** (2016) 1 (DOI: 10.1080/23311916.2016.1138920).
[4] S. Zhang, *et al.*: "Cross-coupled bandpass filter based on circular substrate integrated waveguide resonator," IEICE Electron. Express **13** (2016) 20160953 (DOI: 10.1587/elex.13.20160953).
[5] F. Zhu, *et al.*: "Wide stopband substrate integrated waveguide filter using corner cavities," Electron. Lett. **49** (2013) 50 (DOI: 10.1049/el.2012.3891).
[6] D. Jia, *et al.*: "Multilayer substrate integrated waveguide (SIW) filters with higher-order mode suppression," IEEE Microw. Wireless Compon. Lett. **26** (2016) 678 (DOI: 10.1109/LMWC.2016.2597222).
[7] K. Dhwaj, *et al.*: "Cavity resonators do the trick: A packaged substrate integrated waveguide, dual-band filter," IEEE Microw. Mag. **17** (2016) 58 (DOI: 10.1109/MMM.2015.2487920).
[8] S. Zhang, *et al.*: "A novel dual-band controllable bandpass filter based on fan-shaped substrate integrated waveguide," IEEE Microw. Wireless Compon. Lett. **28** (2018) 308 (DOI: 10.1109/LMWC.2018.2805460).
[9] K. Zhou, *et al.*: "Resonance characteristics of substrate-integrated rectangular cavity and their applications to dual-band and wide-stopband bandpass filters design," IEEE Trans. Microw. Theory Techn. **65** (2017) 1511 (DOI: 10.1109/TMTT.2016.2645156).
[10] X. Guo, *et al.*: "Design method for multiband filters with compact configuration in substrate integrated waveguide," IEEE Trans. Microw. Theory Techn. **66** (2018) 3011 (DOI: 10.1109/TMTT.2018.2830337).
[11] K. Wang, *et al.*: "A novel SIW dual-band bandpass filter on a double-layer substrate using loaded posts," Microw. Opt. Technol. Lett. **58** (2016) 155 (DOI: 10.1002/mop.29511).
[12] X. P. Chen, *et al.*: "Dual-band and triple-band substrate integrated waveguide filters with Chebyshev and quasi-elliptic responses," IEEE Trans. Microw. Theory Techn. **55** (2007) 2569 (DOI: 10.1109/TMTT.2007.909603).
[13] Y. Dong, *et al.*: "Miniaturised multi-band substrate integrated waveguide filters using complementary split-ring resonators," IET Microw. Antennas Propag. **6** (2012) 611 (DOI: 10.1049/iet-map.2011.0448).
[14] S. Xu, *et al.*: "Novel defected ground structure and two-side loading scheme for miniaturized dual-band SIW bandpass filter designs," IEEE Microw. Wireless Compon. Lett. **25** (2015) 217 (DOI: 10.1109/LMWC.2015.2400916).
[15] S. A. Shakib, *et al.*: "A compact triple-band bandpass filter based on half-mode substrate integrated waveguides," 2012 42nd European Microwave Conference (2013) 116 (DOI: 10.23919/EuMC.2012.6459144).
[16] M. Esmaeili, *et al.*: "Substrate integrated waveguide triple-passband dual-stopband filter using six cascaded singlets," IEEE Microw. Wireless Compon. Lett. **24** (2014) 439 (DOI: 10.1109/LMWC.2014.2316242).
[17] R. Camdoo, *et al.*: "Compact cross-coupled half-mode substrate integrated waveguide bandpass filter," 2017 IEEE Asia Pacific Microwave Conference (APMC) (2018) 706 (DOI: 10.1109/APMC.2017.8251544).
[18] C. Y. Zheng, *et al.*: "A compact wideband filter designed on single one-third equilateral triangular cavity," Microw. Opt. Technol. Lett. **58** (2016) 1993 (DOI: 10.1002/mop.29961).
[19] F. Chen, *et al.*: "Compact dual-band bandpass filter using HMSIW resonator and slot perturbation," IEEE Microw. Wireless Compon. Lett. **24** (2014) 686 (DOI: 10.1109/LMWC.2014.2342883).
[20] S. Zhang, *et al.*: "Novel compact single-band and dual-band bandpass filter based on one-third-mode substrate integrated waveguide," IEICE Electron. Express **14** (2017) 20170832 (DOI: 10.1587/elex.14.20170832).
[21] K. Wang, *et al.*: "A novel compact dual-band filter based on quarter-mode substrate integrated waveguide and complementary split-ring resonator," Microw. Opt. Technol. Lett. **58** (2016) 2704 (DOI: 10.1002/mop.30131).
[22] F. Ren, *et al.*: "Design and implementation of an SIW triple-mode filter," Proc. 3rd Asia-Pacific Conf. Antennas Propag. (2014) 1228 (DOI: 10.1109/APCAP.2014.6992738).
[23] D. D. Zhang, *et al.*: "Novel bandpass filters by using cavity-loaded dielectric resonators in a substrate integrated waveguide," IEEE Trans. Microw. Theory Techn. **62** (2014) 1173 (DOI: 10.1109/TMTT.2014.2314677).
[24] C. Jin, *et al.*: "Compact triple-mode filter based on quarter-mode substrate integrated waveguide," IEEE Trans. Microw. Theory Techn. **62** (2014) 37 (DOI: 10.1109/TMTT.2013.2293128).
[25] Z. Liu, *et al.*: "Triple-mode bandpass filters on CSRR loaded substrate integrated waveguide cavities," IEEE Trans. Compon. Packag. Manuf. Technol. **6** (2016) 1099 (DOI: 10.1109/TCPMT.2016.2574562).
[26] H.-Y. Wang, *et al.*: "A novel triple-band filter based on triple-mode substrate integrated waveguide," Progr. Electromagn. Res. Lett. **58** (2016) 59 (DOI: 10.2528/PIERL15102601).
[27] W. L. Tsai, *et al.*: "Triband filter design using laminated waveguide cavity in LTCC," IEEE Trans. Compon. Packag. Manuf. Technol. **4** (2014) 957 (DOI: 10.1109/TCPMT.2014.2319299).
[28] J. D. Baena, *et al.*: "Equivalent-circuit models for split-ring resonators and complementary split-ring resonators coupled to planar transmission lines," IEEE Trans. Microw. Theory Techn. **53** (2005) 1451 (DOI: 10.1109/TMTT.2005.845211).
[29] M. Ohira, *et al.*: "Deterministic extraction of direct source/load coupling and its application to multi-mode filter designs based on transversal array network theory," 2013 IEEE MTT-S International Microwave Symposium Digest (MTT) (2014) 1 (DOI: 10.1109/MWSYM.2013.6697465).
[30] J.-S. G. Hong and M. J. Lancaster: *Microstrip Filters for RF/Microwave Applications* (Wiley, New York, 2001) 257.